AIAA 3rd "Unmanned Unlimited" Technical Conference, Workshop and Exhibit
20 - 23 September 2004, Chicago, Illinois

AIAA 2004-6527

Benefits of Trajectory Optimization in Airship Flights

Yiyuan J. Zhao* William L. Garrard†
University of Minnesota, Minneapolis, MN 55455

and

Joe Mueller‡
Princeton Satellite Systems, Princeton, NJ 12234

Abstract

This paper studies characteristics of optimal airship flight trajectories in the atmosphere. Principles of airship flight are first reviewed. A three-dimensional point-mass model including the effect of added mass is developed. Airship flight from given initial conditions to specified final conditions is formulated as a nonlinear optimal control problem. Performances are selected to minimize the flight time or the energy consumption. Path constraints are imposed on airship states and controls in obtaining optimal flight trajectories. Approximate analytical solutions are obtained under several simplifying assumptions. Then, the original problem is converted into a parameter optimization problem using a collocation approach, and example numerical solutions are obtained. Main features of the numerical solutions are consistent with approximate analytical solutions. The flight times and energy consumptions of the two performance indices are compared.

I. Introduction

Lighter-than-air-vehicles are an attractive solution for many applications requiring a sustained airborne presence. Known as derigibles, blimps, and airships: these buoyant vehicles represent an approach to meeting challenging requirements for which traditional aircraft are not well-suited. Potential applications include roving or hovering surveillance and communication utilities for both military and commercial use and a variety of remote-sensing instruments for the scientific community. In general, airships are safe and economic. They fulfill different roles from those of fixed-wing airplanes and helicopters.

Recent advances in lightweight materials give rise to the feasibility and popularity of airships[1,2], especially unmanned airships. Indeed, a high altitude airship (HAA) employed for surveillance and/or communication relay would have the following attractive features: (1) Lift is provided by a buoyance force and no energy is thus required to maintain vertical position. (2) The large surface area of an airship lends itself to the integration of solar cells for generating power to support its payload; guidance and control system; and propulsion system. (3) The high operational altitude is above cloud formations; enabling direct sunlight to reach the solar cells. (4) An airship would stay in a calm portion of the atmosphere with low wind speeds and would not interfere with commercial air traffic. In addition, a HAA can maintain a geostationary location close to the surface of the earth at any combination of latitude and longitude. In comparison, a geostationary satellite can match only the longitude with a much higher altitude; whereas, several low earth orbit satellites would be required to provide an equivalent continuous coverage.

On the other hand, the combination of a limited energy source and a stringent requirement for long endurance makes it important for the airship to fly energy-efficient trajectories during ascent, descent, and station transfers. At the same time, the unique aerodynamic properties of airships make them much more sensitive to wind and general atmospheric conditions than traditional aircraft. There, the application of trajectory optimization becomes desirable for planning energy-efficient airship flights in the atmosphere.

The importance of optimal airship flight was long appreciated by Munk in 1922[3]. Limited by the navigational equipment available at that time, Munk proposed the strategy of maintaining a great circle arc

* Associate Professor, Aerospace Eng. & Mechanics, Associate Fellow AIAA, gyyz@aem.umn.edu

† Professor and Head, Aerospace Eng. & Mechanics, Associate Fellow AIAA, wgarrard@aem.umn.edu

‡ Research Engineer, jmueller@psatellite.com

course and examined constant airspeeds that can minimize the fuel consumption over a specified range. We could not find other related work in the literature since then.

The purpose of this paper is to gain insights into main characteristics of optimal airship flights in the atmosphere by using methods of dynamic optimization. To develop appropriate problem formulations, basic principles of airship flight are first reviewed. Next, A point-mass airship flight model is developed and proper flight constraints are identified. Airship flights between specified boundary conditions are formulated as optimal control problems and two performance indices are selected. One minimizes the flight time and the other minimizes the total energy consumption between the two locations. Both problems are subject to airship equations of motion and constraints on airship state and control variables. Approximate analytical solutions are obtained for several flight scenarios under simplifying assumptions. To obtain trajectory solutions without these approximations, the formulated optimal control problems are converted into parameter optimization problem via a collocation approach and example numerical solutions are obtained. Main features of minimum flight time trajectories are compared with those of minimum energy flights.

II. Basic Principles of Airship Operation

An airship is a self-powered, lighter-than-air craft. The most distinguishing feature of an airship is that it uses buoyancy to provide most or all of the lift. Usually, it derives its buoyancy from a lighter-than-air gas such as helium or hot air, while it is propelled forward by an engine. The classic design of an airship consists of an axisymmetric, teardrop-shaped hull with gondola located on the underside of the craft, which houses the payload and propulsion system, and a set of large control surfaces located at the rear. Fig. 1 shows a schematic drawing of an airship for illustrative purposes.

In general, all airships fall into one of two categories: pressure airships and rigid airships. In a pressure airship, the shape of the hull is maintained by a pressure differential between the internal lifting gas and the external atmosphere. In rigid airships, the shape is formed by a lightweight outer shell with a fabric skin, while the lifting gas is stored in internal gas bags. The famous Graf Zeppelin II and the Hindenburg were both rigid airships. Pressure airships may also be made semi-rigid by adding a structural keel to share bending loads generated by aerodynamic forces.

In addition, airships may also be characterized by the types of lifting gas used in the envelopes: helium airships and hot air airships. Helium is used as the source of lift in airships because it is inert and non-flammable. Actually helium is an excellent fire extinguisher, which makes the airships very safe. In contrast, hot air airships or thermal airships are elongated traditional hot-air balloons with propulsion engines. Compared to helium airships, hot air airships have lower initial and operational costs, and are easier to store and transport since their envelopes can be deflated after each flight. On the other hand, hot air airships are limited in flight durations and payload capacity. A continuous heat source is required onboard a hot air airship to heat up the air in order to maintain flight. One cubic meter of hot air only lifts 300 grams, which limits the payloads that hot air airships can carry. As a result, hot air airships are mainly used in sports competition, advertising, and environmental work.

Airships can also be categorized into manned airships and radio controlled (RC) airships by means of the operational principles. Most RC airships are non-rigid airships, and their flexible envelopes are kept in shape by internal overpressure. The current research interests on unmanned aerial vehicles have also affected the development of unmannned airships. In particular, high altitude airships used for long duration surveillance and/or communication relays must be made autonomous.

In this paper, only pressure airship designs filled with helium are considered. It is further assumed that airships are operated remotely from the ground. The development of an aerodynamic model and design of feedback control laws for a pressure airship are discussed in Ref. 4.

The upward buoyancy force generated by an airship, called the gross lift, is equal to the weight of the displaced air. Subtracting the weight of the lifting gas (helium), we obtain the net lift. Since the volume of the displaced air is equal to the volume occupied by the helium V_N, the net lift is given by

$$L_N = V_N(\rho - \rho_H)g \tag{1}$$

where ρ is the air density and ρ_H the density of helium. This is the amount of lift available to counteract the weight of the airship and payload. To maintain the vertical equilibrium through the buoyance force alone, the net lift must be equal to the combined weight of the airship structure, systems and payload.

$$L_N = (m_s + m_p)g \tag{2}$$

The densities of both the air and helium vary with altitude. If both gases are at the same pressure and temperature, the densities will change uniformly with altitude. Although a slight pressure differential is required to maintain inflation, it is small enough to be negligible. Therefore, it is assumed that the density of helium changes at the same rate as air density across altitude:

$$\frac{\rho(h)}{\rho(h_s)} = \frac{\rho_H(h)}{\rho_H(h_s)} = \sigma \tag{3}$$

where h_s represents sea-level altitude.

As the density of the helium ρ_H decreases with altitude, the volume V_N must increase in order to provide the needed lift. This is achieved through ballonets, which expand and contract with air to regulate the internal pressure and thus volume. At the launching altitude (e.g. sea level), the ballonets are expanded to their maximum volume, and thus V_N has its minimum value. As the airship rises, the ambient air density and pressure both fall. In order to regulate the amount of lift, air needs to be ejected from the ballonets to match the falling pressure. At some point in the ascent, the ballonets are completely emptied. At this point, no further expansion of the gas space is possible: V_N has reached a maximum value, $V_{N,\max}$. The corresponding altitude is called the **pressure altitude**. Continued ascent can cause a reduction in the net lift as the densities fall but the volume remains constant. The pressure differential will also increase and can cause the rupture of the skin if it becomes too great. Helium may be vented out to avoid rupture, but this is undesirable for long-endurance applications as it reduces the available lift and shortens the mission life. Therefore, it is important to keep the airship below the pressure altitude.

It can be shown that the net lift is roughly constant over all altitudes below the pressure altitude. Since

$$m_H = V_N \rho_H \tag{4}$$

Eq. (1) leads to

$$L_N = \frac{m_H}{\rho_H}(\rho - \rho_H)g = m_H \left(\frac{\rho}{\rho_H} - 1\right) g = m_H \left(\frac{\rho(h_0)}{\rho_H(h_0)} - 1\right) g \tag{5}$$

which is independent of altitude.

At the pressure altitude, $V_N = V_{N,\max}$. Let the density ratio at this altitude be denoted by σ_p. We have

$$V_{N,\max} = \frac{m_H}{\rho_{H,p}} = \frac{m_H}{\sigma_p \rho_H(h_0)} = \frac{V_N(h_0)}{\sigma_p} \tag{6}$$

or

$$V_N(h_0) = \sigma_p V_{N,\max} \tag{7}$$

In other words, the volume of the helium at the sea level relates to its maximum volume through σ_p. At $h = 21$ km, $\sigma_p = 0.061$. The net volume at sea-level is therefore only 6% of the total available volume, or the ballonets must occupy the remaining 94%. This is a difficult inflation ratio to realize.

The above relations may also be used to estimate the desirable shape of an airship. Combining Eqs. (2), (5), (6), we have

$$V_{N,\max} = \frac{m_s + m_p}{\sigma_p(\rho(h_0) - \rho_H(h_0))} \tag{8}$$

which expresses the total required volume of the airship hull as a function of the masses of the airship structure and payload, as well as the altitude-dependent density ratio. At the same time, the airship structural mass depends on the total volume because of the weight of the envelope fabric. Accordingly, a related issue would

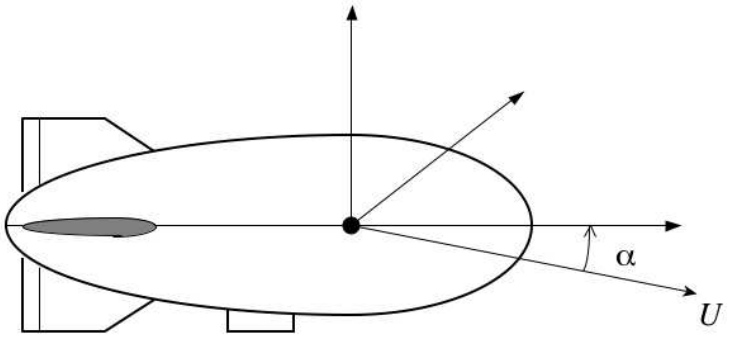

Figure 1 A schematic drawing of an airship.

be to design an appropriate shape of the airship by maximizing the volume while minimizing the structural mass.

The structural mass is the sum of the mass of the external fabric and the remaining mass of the supporting structure and systems. Because the mass of the external fabric is proportional to the surface area, a spherical shape is desirable as it provides the minimum surface area for a given volume. However, a sphere would be a poor choice aerodynamically, as it generates a significant pressure drag. As a result, an ellipsoidal shape represents a compromise between the need to minimize the airship weight and that to reduce the aerodynamic drag. For conceptual designs, the shape of an airship can be approximated as a combination of two ellipsoids, both having the same diameter. The front part is approximated with a shorter ellipsoid, whereas the rear part is approximated by a longer ellipsoid (Figure 1).

III. Airship Equations of Motion

For the purpose of optimal trajectory analysis, a point-mass airship model is used. Several assumptions are first made in order to make the equations of motion tractable. In practice, unmanned airships need to be controlled to follow planned trajectories. The design of appropriate onboard feedback control systems is discussed in Ref. 4. It is assumed in this paper that these control laws perform properly to maintain attitudes required for trajectory tracking. It is further assumed that the buoyance force balances the airship weight, and the airship flies at zero angle of attack, zero sideslip and zero roll. The lift force will be zero as a result. The corresponding equations of motion are given by

$$(m + m_a)\dot{U} = T - D \tag{9}$$

$$\dot{\ell} = \frac{U \cos\gamma \sin\Psi + W_E(\ell, \lambda, h, t)}{(R + h)\cos\lambda} \tag{10}$$

$$\dot{\lambda} = \frac{U \cos\gamma \cos\Psi + W_N(\ell, \lambda, h, t)}{R + h} \tag{11}$$

$$\dot{h} = U \sin\gamma \tag{12}$$

where the airship mass m is assumed constant. In these equations, the control variables are $[T, \Psi, \gamma]$ and state variables are $[U, \ell, \lambda, h]$. This is reasonable since the closed-loop control takes about 10 minutes to reach steady-state values of heading and flight path angle, whereas the typical time interval for the optimization problem is much longer.

A unique feature of airship compared with conventional aircraft is the non-negligible role played by added mass. Any body moving through a fluid displaces that fluid. Because airships displace a significant mass of the air through which they move, it is necessary to account for the effect of the momentum of the

air in developing equations of motion. This results in "added mass" being added to the nominal mass of the airship. In Eq. (9), the added mass along the major axis of an airship is included. This added mass may be estimated as[5]

$$m_a(h) = k_1 \rho(h)\ V_N \tag{13}$$

where k_1 is the airship inertia factor. If an airship is approximated by an ellipsoid with semi-major axis a and semi-minor axis b, we have

$$V_N = \frac{4\pi}{3} a b^2 \tag{14}$$

$$k_1 = \frac{\alpha_0}{2 - \alpha_0} \tag{15}$$

$$\alpha_0 = \frac{1 - e^2}{e^3} \left(\ln \frac{1+e}{1-e} - 2e \right) \tag{16}$$

$$e = \sqrt{a^2 - b^2}/a \tag{17}$$

The aerodynamic drag on an airship needs to be carefully modeled in the study of optimal flights. The most detailed aerodynamic model was found in Jones and DeLaurier[6]. This model includes the expressions for the axial force, normal force, and pitching moment on an axisymmetric airship hull with four equally sized fins: two horizontal and two vertical. Under the assumptions of zero angle of attack, the aerodynamic drag on an airship can be expressed using the standard expression

$$D = \frac{1}{2} \rho S_{\text{ref}} U^2 C_{DV} \tag{18}$$

For airships, it is common to express

$$S_{\text{ref}} = V_N^{2/3} \tag{19}$$

For the example airship model in this paper, the average value of $C_{DV} = 0.027$ is used that corresponds to the Reynolds' number of 1×10^8.

A. Normalized Equations of Motion

To achieve good numerical properties during optimization studies, it is highly desirable to use normalized variables in the optimization iterations. Define characteristic variables

$$d_c = \frac{R}{k^2}, \quad U_c = \frac{\sqrt{gR}}{k}, \quad t_c = \frac{1}{k}\sqrt{\frac{R}{g}}, \quad m_c = m \tag{20}$$

where k is positive number. Variables can then be normalized as

$$\bar{m}_a = \frac{m_a}{m}, \quad \bar{U} = \frac{U}{U_c}, \quad \bar{h} = \frac{h}{d_c}, \quad \tau = \frac{t}{t_c}, \quad \bar{T} = \frac{T}{mg} \tag{21}$$

and

$$(\ )' = \frac{d(\ )}{d\tau} = t_c \frac{d(\ )}{dt} = t_c (\dot{\ }) \quad \Rightarrow \quad (\ )' = \frac{1}{k}\sqrt{\frac{R}{g}} (\dot{\ }) \tag{22}$$

After much algebra, the set of normalized equations of motion are obtained as follows.

$$f^1 = \bar{U}' = \frac{\bar{T} - B_1 \bar{U}^2 \rho(\bar{h})}{1 + B_2 \rho(\bar{h})} \tag{23}$$

$$f^2 = \ell' = \frac{\bar{U} \sin\Psi \cos\gamma + \bar{W}_E(\ell, \lambda, \bar{h}, \tau)}{(k^2 + \bar{h}) \cos\lambda} \tag{24}$$

$$f^3 = \lambda' = \frac{\bar{U} \cos\Psi \cos\gamma + \bar{W}_N(\ell, \lambda, \bar{h}, \tau)}{k^2 + \bar{h}} \tag{25}$$

$$f^4 = \bar{h}' = \bar{U} \sin\gamma \tag{26}$$

where

$$B_1 = \frac{SC_D R}{2mk^2} \tag{27}$$

$$B_2 = \frac{k_1 V_N}{m} \tag{28}$$

$$\bar{W}_E = \frac{W_E}{U_c} \tag{29}$$

$$\bar{W}_N = \frac{W_N}{U_c} \tag{30}$$

B. Typical Motion Constraints

An airship can only operate within its performance limitations. These limitations constitute path constraints on the state and control variables of optimal airship flights. Typically, we have

$$\bar{U}_{\min} \le \bar{U} \le \bar{U}_{\max}, \quad |\lambda| \le \lambda_{\max}, \quad \bar{h}_{\max} \ge \bar{h} \ge 0 \tag{31}$$

$$0 \le \bar{T} \le \bar{T}_{\max}, \quad |\gamma| \le \gamma_{\max}, \quad |\Psi'| \le \Psi'_{\max}, \quad |\gamma'| \le \gamma'_{\max} \tag{32}$$

IV. Modeling of Air Density and Atmospheric Winds

Atmospheric conditions play a key role on the performance capabilities and flight strategies of an airship and thus influence its design. In particular, two atmospheric quantities directly affect optimal airship flight trajectories: air density variation as a function of altitude and wind patterns.

In general, the air density depends on altitude, latitude, longitude, and the time of the year. It can also exhibit considerable fluctuations. In this paper, the air density is assumed to be a function of altitude alone, described by the standard atmosphere conditions. The standard atmosphere from the surface of the Earth to a typical airship operational altitude (e.g. $70,000$ ft) consists of a series of regions of two basic types[7]: isothermal regions and gradient regions. In an isothermal region, the temperature is roughly constant over altitude and the pressure variation with altitude can be described by

$$\frac{p}{p_1} = \frac{\rho}{\rho_1} = e^{-[g_0/(R_a T)](h-h_1)} \tag{33}$$

In a gradient region, the temperature varies linearly with respect to altitude

$$T = T_1 + a(h - h_1) \tag{34}$$

and the pressure variation over altitude is given by

$$\frac{p}{p_1} = \left(\frac{T}{T_1}\right)^{-g_0/(aR_a)}, \quad \frac{\rho}{\rho_1} = \left(\frac{T}{T_1}\right)^{-[g_0/(aR_a)+1]} \tag{35}$$

Air density as a function of altitude can then be obtained by piecing different regions together. The first region in the standard atmosphere is a gradient region from the sea level to 11 km with a lapse rate of -6.5 K per km, followed by an isothermal region from 11 km to 25 km with a constant temperature of 216.66, followed by another gradient region from 25 to 47 km with the lapse rate of 3.0 K per km, and followed by another isothermal region from 47 km to 53 km. This covers sufficient altitude range for the current airship trajectory planning problem.

To help the convergence of trajectory optimization process, the standard atmosphere air density function is calculated at a series of altitudes and approximated by a fifth order polynomial of the normalized altitude. Mathematically,

$$\rho(\bar{h}) = b_0 + b_1\bar{h} + b_2\bar{h}^2 + b_3\bar{h}^3 + b_4\bar{h}^4 + b_5\bar{h}^5 \tag{36}$$

Models of wind patterns directly affect characteristics of the resulting optimal trajectories. However, the wind velocities on Earth can be highly variable. Because airship flight speeds are usually small, the accurate determination of wind velocities can be an essential aspect of applying optimal flight strategies in practice. The main purpose of this paper is to establish basic problem formulations in the design of optimal flight trajectories and to examine fundamental features of these flights. Therefore, wind models are developed based on documented measurements of actual wind patterns. Specific wind models will be presented in the section of numerical results.

V. Problem Formulations of Optimal Airship Flight

There are two important performance concerns in designing airship flight trajectories: flight time and energy consumption over a specified range. Therefore, an optimal control problem is formulated that seeks to minimize a linear combination of the flight time and the energy consumption between specified boundary conditions.

The power required from an electric motor to generate a thrust of T at an airspeed of U on a propeller is given by

$$P_{\text{req}} = TU/\eta_p/\eta_e \tag{37}$$

where η_e is the efficiency of the electric motors and η_p is the propulsive efficiency of the propellers. The electric motor efficiency η_e is independent of airship flight speed. While the propulsive efficiency η_p of the propellers is in general a function of the airship flight speed, it may be assumed also to be relatively independent of the airship flight speed for a wide range of flight speed. As a result, the optimization of airship flight can be stated mathematically as

$$\min_{\bar{T},\Psi',\gamma';\tau_f} \quad I = K_t\tau_f + K_p\int_0^{\tau_f} \bar{T}\bar{U}d\tau \tag{38}$$

subject to the normalized equations of motion in Eqs. (23) through (26), path constraints on states and controls in Eqs. (31) and (32), the following initial conditions

$$\bar{U}_I(0) = \bar{U}_{I0} \tag{39}$$
$$\Psi_I(0) = \Psi_{I0} \tag{40}$$
$$\gamma_I(0) = \gamma_{I0} \tag{41}$$
$$\bar{h}(0) = \bar{h}_0 \tag{42}$$
$$\ell(0) = \ell_0 \tag{43}$$
$$\lambda(0) = \lambda_0 \tag{44}$$

and the following terminal constraints

$$\bar{U}_I(\tau_f) = \bar{U}_{If} \tag{45}$$
$$\Psi_I(\tau_f) = \Psi_{If} \tag{46}$$
$$\gamma_I(\tau_f) = \gamma_{If} \tag{47}$$
$$\bar{h}(\tau_f) = \bar{h}_f \tag{48}$$
$$\ell(\tau_f) = \ell_f \tag{49}$$
$$\lambda(\tau_f) = \lambda_f \tag{50}$$

where inertial velocity components relate to air velocity components through

$$\bar{U}_I\cos\gamma_I\sin\Psi_I = \bar{U}\cos\gamma\sin\Psi + \bar{W}_E \tag{51}$$
$$\bar{U}_I\cos\gamma_I\cos\Psi_I = \bar{U}\cos\gamma\cos\Psi + \bar{W}_N \tag{52}$$
$$\bar{U}_I\sin\gamma_I = \bar{U}\sin\gamma \tag{53}$$

and the time rate of change of distance is given by

$$\bar{s}' = \bar{U}_I, \quad \text{where } \bar{s} = \frac{s}{d_c} \tag{54}$$

By selecting $K_t = 1$, $K_p = 0$, a minimum-time trajectory can be obtained, and by selecting $K_t = 0$, $K_p = 1$, a minimum power consumption trajectory results. In addition, a fixed final time minimum energy problem can also be examined by specifying $K_t = 0$ and $K_p = 1$ with the final time τ_f fixed.

In the conventional optimal control theory, Ψ and γ should be state variables in order to enforce the boundary conditions in Eqs. (40), (41), (46), and (47). This can be done by defining their derivatives control variables. This would require adding two more differential equations to the system dynamics in Eqs. (23) through (26). In this paper, a parameterization-based approach is used to obtain numerical solutions, where both state and control variables are approximated by a set of parameters. As a result, constraints on both states and controls can be directly enforced. Computational experiences indicate that the resulting trajectories are the same as those obtained by defining Ψ and γ as states.

VI. Approximate Analytical Solutions

In general, the above problem can only be solved numerically. Under appropriate assumptions, approximate analytical solutions can be obtained and these analytical solutions provide useful insights into the fundamental characteristics of the optimal solutions.

Assuming $\cos\gamma \approx 1$ and $h \ll R$, the Eqs. (24) and (25) become

$$\ell' = \frac{\bar{V}\sin\Psi + \bar{W}_E}{k^2\cos\lambda} = \frac{\bar{V}\sin\Psi + \bar{V}_w\sin\Psi_w}{k^2\cos\lambda} \tag{55}$$

$$\lambda' = \frac{\bar{V}\cos\Psi + \bar{W}_N}{k^2} = \frac{\bar{V}\cos\Psi + \bar{V}_w\cos\Psi_w}{k^2} \tag{56}$$

A. Great Circle Arcs

Great circle arc represents the shortest geometric path between a pair of specified locations on earth. A great circle arc solution can actually be obtained by assuming that the flight speed is constant and there is no wind. In this case, the minimum distance flight is the same as the minimum-time flight. Using longitude ℓ as the independent variable, the minimum-time problem becomes

$$\min_{\Psi} \quad I = \int_{\ell_0}^{\ell_f} \frac{\cos\lambda}{\sin\Psi} d\ell \tag{57}$$

subject to

$$\frac{d\lambda}{d\ell} = \cos\lambda\frac{\cos\Psi}{\sin\Psi} \tag{58}$$

where (ℓ_0, λ_0) and (ℓ_f, λ_f) are specified.

Analytical solution to this problem for the Northern Hemisphere is derived in Bryson[8] and is repeated here for convenience. The optimal heading history is given by

$$\sin\Psi = \frac{\cos\lambda_m}{\cos\lambda} \tag{59}$$

where λ_m is the maximum latitude, and can be determined from

$$\tan\ell_m = \frac{\tan\lambda_0\cos\ell_f - \tan\lambda_f\cos\ell_0}{\sin\ell_0\tan\lambda_f - \sin\ell_f\tan\lambda_0} \tag{60}$$

and

$$\tan\lambda_m = \frac{\tan\lambda_0}{\cos(\ell_m - \ell_0)} = \frac{\tan\lambda_f}{\cos(\ell_m - \ell_f)} \tag{61}$$

It is noted that great circle arc solutions may not be optimal in the presence of horizontal winds. These solutions may be used as comparison trajectories to determine the benefits of wind-optimal solutions.

B. Optimal Variable Speed for Given Heading History

If the great circle arc between two specified locations is followed, the airship may vary its flight speed to minimize the energy consumption for the trip. Assuming the flight speed control is quasi-instantaneous: $\bar{T} = B_1 \bar{V}^2 \rho(\bar{h})$, the optimal flight speed can be determined by minimizing the instantaneous energy rate per unit flight distance

$$\begin{aligned}\min_{\bar{V}} \frac{dE}{ds} &= \frac{\bar{T}\bar{V}}{\sqrt{\bar{V}^2 + 2\bar{V}\bar{V}_w \cos\gamma \cos(\Psi - \Psi_w) + \bar{V}_w^2}} \\ &= B_1 \rho(\bar{h}) \cdot \frac{\bar{V}^3}{\sqrt{\bar{V}^2 + 2\bar{V}\bar{V}_w \cos\gamma \cos(\Psi - \Psi_w) + \bar{V}_w^2}} \\ &= B_1 \rho(\bar{h}) \bar{V}_w^2 \frac{v^3}{\sqrt{v^2 + 2v\cos\gamma\cos\Delta\Psi + 1}} = B_1 \rho(\bar{h}) \bar{V}_w^2 \cdot I \end{aligned} \tag{62}$$

where

$$v = \frac{\bar{V}}{\bar{V}_w} \qquad \Delta\Psi = \Psi - \Psi_w \tag{63}$$

and

$$I = \frac{v^3}{\sqrt{v^2 + 2v\cos\gamma\cos\Delta\Psi + 1}} \approx \frac{v^3}{\sqrt{v^2 + 2v\cos\Delta\Psi + 1}} \tag{64}$$

Note that

$$v^2 + 2v\cos\Delta\Psi + 1 = (v + \cos\Delta\Psi)^2 + (\sin\Delta\Psi)^2 \geq 0 \tag{65}$$

The problem of selecting the best flight speed at a given heading becomes

$$\min_{v \geq 0} \; I = \frac{v^3}{\sqrt{v^2 + 2v\cos\Delta\Psi + 1}} \tag{66}$$

The derivative of the cost function is given by

$$\begin{aligned}\frac{\partial I}{\partial v} &= \frac{2v^2(v^2 + 2.5v\cos\Delta\Psi + 1.5)}{(v^2 + 2v\cos\Delta\Psi + 1)^{3/2}} \\ &= \frac{2v^2(v - v_1)(v - v_2)}{(v^2 + 2v\cos\Delta\Psi + 1)^{3/2}} \end{aligned} \tag{67}$$

where

$$v_1 = 1.25\left[-\cos\Delta\Psi - \sqrt{\cos^2\Delta\Psi - 6/6.25}\right] \tag{68}$$

$$v_2 = 1.25\left[-\cos\Delta\Psi + \sqrt{\cos^2\Delta\Psi - 6/6.25}\right] \tag{69}$$

If v_1 and v_2 are complex numbers, the derivative is always non-negative, and the minimum value of I occurs at $v = 0$. If v_1 and v_2 are real numbers, on the other hand, the local minimum of I occurs at $v = v_2$. Therefore,

$$v^* = \arg\min I = \begin{cases} 0 & \cos\Delta\Psi > -\sqrt{6/6.25} \\ v_2 & \cos\Delta\Psi \leq -\sqrt{6/6.25} \end{cases} \tag{70}$$

where

$$\cos\Delta\Psi \leq -\sqrt{6/6.25} \Rightarrow 180 - \beta \leq \Psi - \Psi \leq 180 + \beta \tag{71}$$

with $\beta = \cos^{-1}\sqrt{6/6.25} = 11.54$ deg. This solution is consistent with the approximate analytical solution obtained by Munk[3].

C. Minimum Time Climb Trajectory

Sometimes, an airship needs to ascend to a desired altitude as quickly as possible where there is no requirement on the final horizontal location. Assuming constant airspeed and using the flight path angle γ as a control variable, an optimal control problem can be stated as

$$\min_{\gamma,\tau_f} \; I = \tau_f = \int_0^{\tau_f} 1 \; d\tau \tag{72}$$

subject to Eq. (27), the constraint on γ in Eq. (34), and the boundary condition

$$\bar{h}_0 \longrightarrow \bar{h}_f \tag{73}$$

Clearly, the solution to this problem is a bang type and requires the airship to climb using the maximum possible flight path angle.

If the airspeed is varied and assumed as a control variable, the minimum-time climb would result in a decreasing airspeed profile as the airship climbs. In other words, the airship would use both propulsive energy and kinetic energy to reach a desired altitude in the shortest possible time. Details are omitted.

D. Minimum Energy Climb Trajectory

We now examine the question of airship climb from an initial altitude to a desired final altitude using the least amount of energy. It is assumed that the airspeed control is quasi-instantaneous through the use of thrust. We have

$$\bar{T} = B_1 \bar{V}^2 \rho(\bar{h}) \tag{74}$$

and the power required is given by

$$\bar{P} = \bar{T}\bar{V} = B_1 \bar{V}^3 \rho(\bar{h}) \tag{75}$$

We first consider a constant speed climb with a fixed flight time, where the final time is dictated by the requirement to reach a specified horizontal location. The problem of minimum energy climb can be stated as

$$\min_{\gamma} \; I = \int_0^{\tau_f} \rho(\bar{h}) \; d\tau \tag{76}$$

subject to Eq. (26), the bound on γ in Eq. (32), the boundary condition in Eq. (73), and the maximum altitude constraint in Eq. (31).

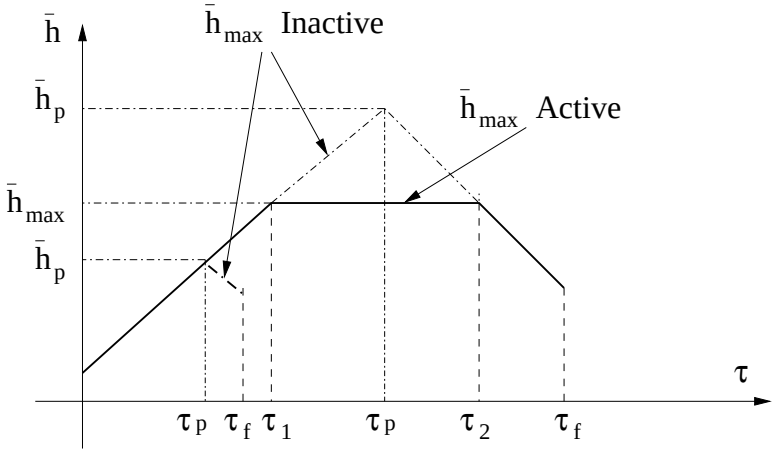

Figure 2 Optimal vertical climb trajectory structure.

While detailed solution process is omitted for brevity, an optimal vertical trajectory structure is identified as shown in Figure 2. In the optimal solution, the airship would first climb until reaching the maximum altitude constraint. It would then stay at the maximum altitude and descend to the final altitude toward the end. If the maximum altitude constraint is sufficiently high, the airship would climb to a peak altitude and then immediately descend to the desired altitude. This is because the density is lower at a higher altitude, thus climbing to a higher altitude would enable the airship to lower the performance index in Eq. (76).

In fact, the above strategy also minimizes the flight time if it is open. The quickest climb portion in Figure 2 is consistent with the minimum-time climb strategy when there is no constraint on the final horizontal location. If the final horizontal location is specified, on the other hand, a longer flight time may be needed to arrive at the specified location. In this case, the optimal solution structure in Figure 2 minimizes both the flight time and the energy consumption.

Finally, let us consider the case when the airspeed can vary. In this case, the airspeed is used as a control variable and the problem of minimum energy climb is stated as

$$\min_{\bar{V},\gamma} \quad I = \int_0^{\tau_f} \bar{V}^3 \rho(\bar{h})\ d\tau \tag{77}$$

subject to Eq. (26), the bound on γ in Eq. (32), the boundary condition in Eq. (73), and the path constraints in Eq. (31).

When the maximum altitude constraint is not active, the Hamiltonian function can be defined as

$$H = \rho(\bar{h})\bar{V}^3 + \Gamma \bar{V} \sin\gamma = \text{constant} \tag{78}$$

where Γ is the Lagrange multiplier function. We have

$$\gamma = -\gamma_{\max}\ \text{sgn}(\Gamma) \tag{79}$$

and

$$0 = H_{\bar{V}} = 3\rho(\bar{h})\bar{V}^2 + \Gamma \sin\gamma = 3\rho(\bar{h})\bar{V}^2 - \sin\gamma_{\max}|\Gamma| = 0 \tag{80}$$

where

$$\Gamma' = -H_{\bar{h}} = -\bar{V}^3 \frac{\partial \rho}{\partial \bar{h}} > 0 \tag{81}$$

Eq. (81) suggests a similar altitude trajectory trend as predicted in the above. Substituting Eqs. (79) and (80) into Eq. (78) leads to

$$H = \rho(\bar{h})\bar{V}^3 - \bar{V} \sin\gamma_{\max}|\Gamma| = -2\rho(\bar{h})\bar{V}^3 = \text{constant} \tag{82}$$

Therefore

$$\frac{\bar{V}^*(\bar{h}_1)}{\bar{V}^*(\bar{h}_2)} = \left[\frac{\rho(\bar{h}_2)}{\rho(\bar{h}_1)}\right]^{\frac{1}{3}} \tag{83}$$

Clearly as altitude increases, the air density decreases and the optimal airspeed increases.

VII. Numerical Solution Methods

In general, the optimal control problem formulated in Eq. (39) can only be solved numerically. In this paper, a collocation approach[9] is used to obtain numerical solutions, in which both state and control variables are parameterized. Differential equations are enforced as a system of nonlinear constraints through a forward difference scheme, in which state equations are evaluated at the middle of the nodes. This method results in piecewise constant control histories and piecewise linear state histories. The terminal constraints are treated as nonlinear constraints. The resulting parameter optimization problems are solved with the software program NPSOL[10]. In using NPSOL, analytical gradient expressions are provided for all constraints as well as the objective functions.

Strictly speaking, computed optimal trajectories only represent approximations to solutions of the original problems. These approximations normally approach to the original solutions as the number of nodes becomes large. However when N is too large, it is found that not only the computational process takes a

long time, it is also more difficult to obtain a converged solution from simple initial guesses. In the results presented below, $N = 31$ is used.

VIII. Numerical Results

Consider a flight scenario in which an airship flies over New York City, starting from an initial altitude of 18 km and reaching an operating altitude of $h_{\rm cr} = 21.5$ km. The maximum feasible altitude is assumed to be $h_{\max} = 22.5$ km. The following initial airship states are specified as

$$\ell(0) = -73.98^o,\ \lambda(0) = 40.77^o,\ h(0) = 18.0 \text{ km},\ V_I(0) = 33 \text{ m/s},\ \Psi_I(0) = 93^o,\ \gamma_I(0) = 0^o \tag{84}$$

and the final conditions are specified as

$$h(t_f) = 21.4 \text{ km},\ V_I(t_f) = 7 \text{ m/s},\ \Psi_I(t_f) = -84^o,\ \gamma_I(t_f) = 0^o \tag{85}$$

These boundary conditions specify that the airship would start out east, and then climbs and heads west. The final horizontal position is not specified.

The wind components on January 9, 2004 between 18 km to 22.5 km can be reasonably approximated by linear functions of altitude.

$$W_E = 45.96 - 1.5686 \times 10^{-3} h \text{ m/s} \tag{86}$$

$$W_N = 2.05 - 0.1616 \times 10^{-3} h \text{ m/s} \tag{87}$$

To obtain examples of optimal airship flights, the following path constraint bounds are imposed:

$$T_{\max} = 0.05\ W, h_{\max} = 22.5 \text{ km}, \gamma_{\max} = 60 \text{ deg}$$

$$\dot{\Psi}_{\max} = 1 \text{ deg/s}, \dot{\gamma}_{\max} = 2 \text{ deg/s} \tag{88}$$

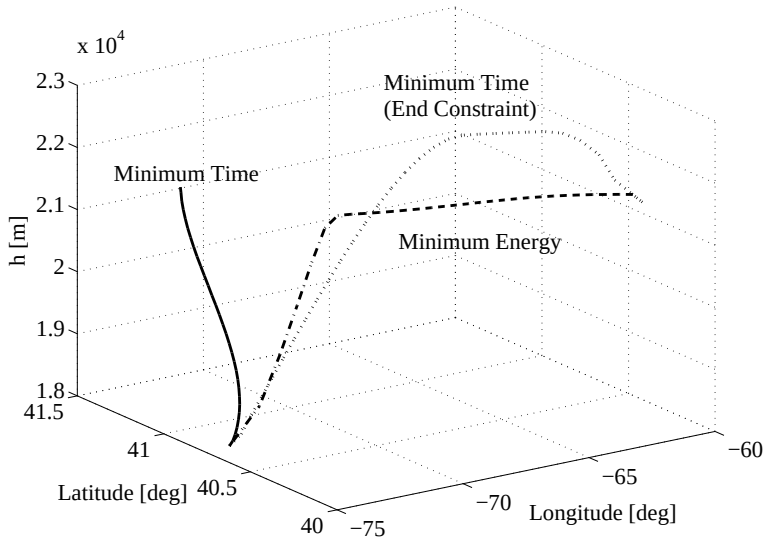

Figure 3 Three-dimensional view of optimal airship trajectories.

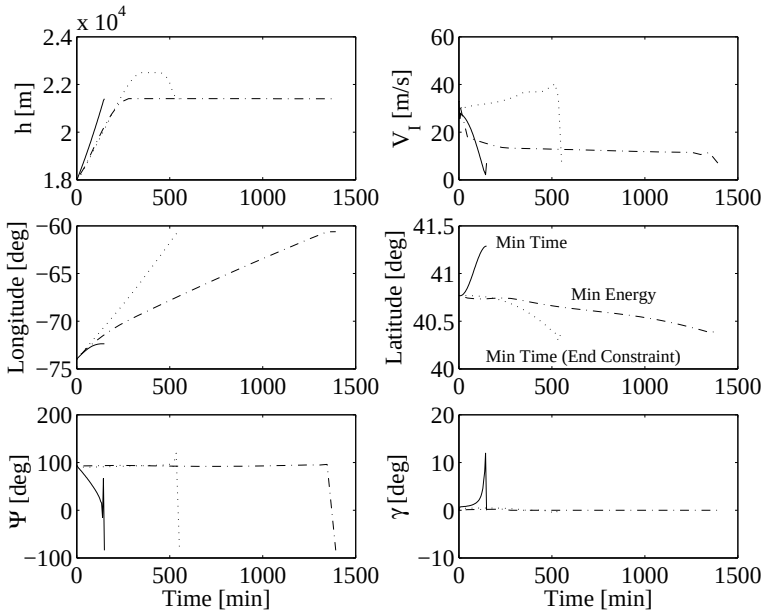

Figure 4 States and controls of optimal airship flights.

Three numerical results are obtained and discussed below.

(1) Minimum-time climb trajectory is first obtained by solving the problem in Eq. (39) with $K_t = 1$, $K_p = 0$, and terminal constraints in Eqs. (45) through (48) without the specification of a final horizontal position. Figures 3 and 4 show the resulting minimum-time optimal ascent trajectory. The numerical solution obtained is consistent with the approximate analytical solution in this case. Particularly, the altitude increases monotonically and the airspeed decreases, in part to satisfy the terminal constraints in Eqs. (85).

(2) Next, the minimum energy climb trajectory is obtained by solving the problem in Eq. (39) with $K_t = 0$ and $K_p = 1$. Again, no final horizontal position is specified. The resulting trajectory is also shown in Figures 3 and 4. In this case, the altitude history is basically consistent with the corresponding approximate analytical solutions, except that the airship does not climb all the way to the maximum altitude. Instead, it climbs to and stays at the final desired altitude. This is because when the dynamic airspeed variation is included, it would require additional energy consumption for the airship to climb to the maximum altitude and then descend to the desired final altitude. Still, the trend predicted by the analytical solution that it is more economical for the airship to reach a higher altitude sooner is confirmed.

(3) Finally, we consider the problem of minimum time climb with a specified final horizontal location. In this case, $K_t = 1$ and $K_p = 0$ in Eq. (39). In addition, the final horizontal position is specified through Eqs. (49) and (50) where the desired final position is the same as the one obtained in the above minimum energy climb problem. The resulting optimal climb trajectory is shown in Figures 3 and 4. This optimal trajectory is consistent with the corresponding analytical predictions. Specifically, the airship climbs to the maximum permitted altitude rapidly and descend to the final desired altitude toward the end. During the climb, the airspeed gradually increases until toward the end, where the airship needs to slow down to satisfy the final airspeed constraint in Eq. (85).

Table 1 summarizes the required flight times and the corresponding normalized energy consumptions of the three computed optimal trajectories, where the energy consumption for the minimum energy climb is defined as one. This comparison clearly shows the significant tradeoff between flight time and energy consumption by employing different flight strategies. Comparing the first two cases, an airship can spend about 10 times more energy to reach a desired altitude using about 10th of the time, or vice versa. When the final horizontal position is also specified as in the last two cases, the airship can arrive at the desired final destination with less then half the time of the minimum energy flight, but with about 20 times more energy. Therefore, it is important to employ appropriate flight strategies commensurate with the intended flight objectives in flying the airship.

Tables

Table 1 Comparison of Optimal Trajectory Benefits.

	Flight Time (hrs)	Normalized Energy
Min Time	2.5	11.0
Min Energy	23.2	1.0
Min Time with End Constraint	9.2	19.8

IX. Conclusions

In this paper, airship flight in the atmosphere from a given location to a desired final destination is formulated as nonlinear optimal control problems. A three-dimensional point-mass airship model is developed and the effect of added mass is included. Two performance indices are considered. The first one minimizes the flight time between specified locations, whereas the second one minimizes the energy consumption for the flight. Approximate analytical solutions are first obtained for several special flight scenarios under simplifying assumptions. Numerical methods are then used to obtain more accurate trajectory solutions. These numerical solutions are consistent with the analytical results.

Obtained optimal trajectories indicate that a considerable tradeoff between flight time and energy consumption can be made. Specifically, an airship can arrive at a desired final destination with a much higher energy consumption than a minimum energy flight, which in turn can take a significantly longer flight time. Therefore, this study suggests that an appropriate flight strategy should be devised in consistence with intended flight objectives.

Aknowledgments

The first author, Yiyuan J. Zhao, would like to thank the very helpful discussions with Anthony Colozza.

References

[1] Khoury, G.A., and J.D. Gillett *Airship Technology*, Cambridge Aerospace Series: 10, 1999.

[2] Colozza, A., "Initial Feasibility Assessment of a High Altitude Long Endurance Airship," NASA CR-2003-212724, December 2003,

[3] Munk, Max M., "The Choice of The Speed of An Airship", Technical Notes, National Advisory Committee for Aeronautics, March 1992. http://nasa.larc.gov/reports/1924.

[4] Mueller, J. B., and Zhao, Y, J., "Development of an Aerodynamic Model and Control Law Design for a High Altitude Airship," AIAA 3rd "Unmanned Unlimited" Technical Conference, Workshop and Exhibit, Chicago, Sept. 20-23, 2004.

[5] Milne-Thomson, L. M., *Theoretical Hydrodynamics*, fourth edition, The MacMillan Company, New York, 1960, p. 238.

[6] Jones, S.P., and J.D. DeLaurier,"Aerodynamic Estimation Techniques for Aerostats and Airships", presented at the AIAA Lighter-than-Air Systems Conference, Annapolis, MD, July 1981.

[7] Anderson, J. D., *Introduction to Flight*, 5th edition, McGraw Hill, 2004.

[8] Bryson, A. E., Jr.., *Dynamic Optimization*, Prentice Hall, Addison-Wesley, Inc., 1999.

[9] Hull, D., "Conversion of Optimal Control Problems Into Parameter Optimization Problems." *J. of Guidance, Control, and Dynamics*, Vol. 20, No. 1, 1997, pp. 57-60.

[10] Gill, P. E., Murray, W., Saunders, M. A., and Wright, M. H. , "User's Guide for NPSOL (Version 4.0): A Fortran Package for Nonlinear Programming, " Technical Report SOL 86-2, 1986.